The Muscle Chloride Channel ClC-1 Has a Double-Barreled Appearance that Is Differentially Affected in Dominant and Recessive Myotonia

Chiara Saviane, Franco Conti, and Michael Pusch

From the Istituto di Cibernetica e Biofisica, CNR, I-16149 Genova, Italy

ABSTRACT Single-channel recordings of the currents mediated by the muscle Cl^- channel, ClC-1, expressed in *Xenopus* oocytes, provide the first direct evidence that this channel has two equidistant open conductance levels like the *Torpedo* ClC-0 prototype. As for the case of ClC-0, the probabilities and dwell times of the closed and conducting states are consistent with the presence of two independently gated pathways with ≈1.2 pS conductance enabled in parallel via a common gate. However, the voltage dependence of the common gate is different and the kinetics are much faster than for ClC-0. Estimates of single-channel parameters from the analysis of macroscopic current fluctuations agree with those from single-channel recordings. Fluctuation analysis was used to characterize changes in the apparent double-gate behavior of the ClC-1 mutations I290M and I556N causing, respectively, a dominant and a recessive form of myotonia. We find that both mutations reduce about equally the open probability of single protopores and that mutation I290M yields a stronger reduction of the common gate open probability than mutation I556N. Our results suggest that the mammalian ClC-homologues have the same structure and mechanism proposed for the *Torpedo* channel ClC-0. Differential effects on the two gates that appear to modulate the activation of ClC-1 channels may be important determinants for the different patterns of inheritance of dominant and recessive ClC-1 mutations.

KEY WORDS: ClC-0 • fast gate • slow gate • subconductance

INTRODUCTION

ClC proteins represent a class of voltage-dependent Cl^- channels with several members involved in hereditary human diseases. The Cl^- channel prototype ClC-0 from *Torpedo* is a dimeric protein behaving as if comprising two protopores that can gate independently from each other and a common gate that acts on both protopores (Miller, 1982; Middleton et al., 1996; Ludewig et al., 1996). Such behavior, suggestive of a "double-barreled" structure, has not been demonstrated for other ClC proteins at the single channel level. Indeed, a double-barreled structure of ClC-1 has recently been challenged (Fahlke et al., 1998).

Using single channel recording, we show that also the muscle Cl^- channel, ClC-1, has two equidistant open conductance levels of ≈1.2 and 2.4 pS whose open probability and kinetics are consistent with the presence of two independently gated conductance states modulated in parallel by a common gate, although the relatively fast kinetics of the common gate render their separation less obvious than for ClC-0. We verified that the most simple scheme implementing a double-gate two-protopores model fits well the single-channel data and predicts, for the same single-channel parameters, current fluctuations consistent with macroscopic measurements. Several mutations of ClC-1 causing dominant myotonia lead to a positive shift of the voltage dependence of the conductance that is only partially reversed in mutant/wild-type (WT)[1] heterodimers (Pusch et al., 1995b). We have used macroscopic fluctuation analysis to characterize changes in the double-gate behavior of two mutations of ClC-1 causing dominant or recessive myotonia. Mutation I290M, causing a positive shift of the voltage dependence of the conductance that is only partially reversed in mutant/WT heterodimers (Pusch et al., 1995b), shows a strong reduction of the open probability of the common gate. In contrast, we found that for mutation I556N, which causes a recessive or benign form of dominant myotonia and does not impose its "shift" on WT/mutant heterodimers (Kubisch et al., 1998), the open probability of the common gate is reduced less dramatically.

Our results suggest that the mammalian ClC homologues have the same double-barreled structure as the *Torpedo* channel ClC-0. In addition, our findings for re-

Address correspondence to Michael Pusch, Istituto di Cibernetica e Biofisica, CNR, Via de Marini 6, I-16149 Genova, Italy. Fax: 39 010 6475 500; E-mail: pusch@barolo.icb.ge.cnr.it

[1] *Abbreviation used in this paper:* WT, wild type.

cessive and dominant mutations raise the possibility that, for other mutations also, the pattern of inheritance may derive from differential effects on the double-gate mechanism of ClC-1 activation.

METHODS

Electrophysiology

Channels were expressed in *Xenopus* oocytes and currents were measured at 18°C 2–5 d after injection using the inside-out configuration of the patch clamp technique (Hamill et al., 1981). Bath solution contained (mM): 120 *N*-methyl-D-glucamine (NMDG)-Cl, 2 $MgCl_2$, 5 HEPES, 2 EGTA, pH 7.3 or 6.5. Extracellular (pipette) solution contained (mM): 100 NMDG-Cl, 5 $MgCl_2$, 5 HEPES, pH 7.3. Data were low-pass filtered at one third of the sample frequency. Mutant I290M is described in Pusch et al. (1995b), and mutant I556N in Kubisch et al. (1998). RNA synthesis and oocyte injection were performed as described (Wollnik et al., 1997).

Data Analysis

Single channels were analyzed as described (Ludewig et al., 1996, 1997). Amplitude histograms were fitted with the sum of three gaussian distributions with means i_0, $i_0 + i_1$ and $i_0 + 2i_1$ and with variances σ_0^2, $\sigma_0^2 + \sigma^2$, $\sigma_0^2 + 2\sigma^2$, where i_0 and σ_0^2 are the mean and variance of the leakage current in the patch; i_1 and σ^2 are the mean and variance of the current flowing through a single pore.

Dwell-times of the three conductance levels were fitted on the basis of Scheme B (see Fig. 3) with the four rate constants (α, β, λ, μ) as free parameters using maximum likelihood techniques (Colquhoun and Hawkes, 1995): the two open conductance levels are associated with a single kinetic state; thus, the dwell-time distributions are given by

$$f_i(t) = \frac{1}{\tau_i}\exp(-t/\tau_i)$$

i = 1, 2, with $\tau_1 = 1/(\alpha + \beta + \mu)$; $\tau_2 = 1/(2\beta + \mu)$.

The closed level is associated with four kinetic states, and therefore the distribution is given by

$$f_0(t) = \sum_{j=1}^{4} a_j\lambda_j\exp(-\lambda_j t); \qquad \sum_{j=1}^{4} a_j = 1,$$

where the eigenvalues λ_i and the coefficients a_i are functions of all rate constants. The overall log-likelihood for the observed dwell-times is given by

$$\ln[L(\theta)] = \sum_{i=0}^{2}\sum_{j=1}^{n_i}\frac{f_i(t_{ij}|\theta)}{prob(t_{\min} <= t_{ij} <= t_{\max}|\theta)},$$

where θ denotes the rate constants, n_i is the number of events in level i, t_{ij} is the j^{th} dwell time in level i, and the denominator is the probability that the observed events will fall in the experimental time range. t_{min} was set to 5 ms. The log-likelihood was calculated numerically and maximized by varying the rate constants using the simplex algorithm.

The noise analysis (see Figs. 5 and 6) was performed as follows. From repeated voltage stimulations, from an activating positive voltage to a negative "test" voltage, the mean current, $<I(t)>$, and the variance, $<\sigma^2(t)>$, were calculated (Pusch et al., 1994). The capacity transient was measured from the response to a step to 0 mV; i.e., close to the reversal potential, and subtracted off line. Leakage currents were estimated exploiting the strong rectification of ClC-1 [$|I(-100\text{ mV})|/I(+100\text{ mV})] \approx 8.5$, measured from patches with large expression where the contribution of leakage currents was negligible; when a weaker rectification was measured in a given patch, the leakage current was estimated assuming a linear leakage conductance with a reversal potential of 0 mV.

Assuming their independence, the "fast" and "slow" gates of Fig. 3 were modeled as having time-dependent open probabilities given by:

$$P_f(t) = P_f[1 + a_f\exp(-t/\tau_f)];\ P_s(t) = P_s[1 + a_s\exp(-t/\tau_s)], \quad (1)$$

with initial values $P_f(0) = P_f(1 + a_f)$ and $P_s(0) = P_s(1 + a_s)$, steady state values P_f and P_s, and time constants τ_f and τ_s. Accordingly, the mean current was fitted by

$$<I(t)> = 2niP_f(t)P_s(t) = I_\infty[1 + a_f\exp(-t/\tau_f)][1 + a_s\exp(-t/\tau_s)], \quad (2)$$

where n is the number of channels, i is the single channel current, and $I_\infty = 2niP_fP_s$. The expected time course of the variance according to the scheme of Fig. 3 is given by (Conti, 1984):

$$<\sigma^2(t)> = i<I(t)>\{1 + P_f[1 + a_f\exp(-t/\tau_f)] - <I(t)>/(ni)\}. \quad (3)$$

Eq. 3 was fitted to the measured variance using i, n, and P_f as free parameters. The fit was constrained by imposing that all the resulting estimates of the open probabilities,

$$P_f;\ P_f(0) = P_f(1 + a_f);\ P_s = I_\infty/(2niP_f);\ P_s(0) = P_s(1 + a_s),$$

had to be in the range [0...1]. In most cases, this constraint led to a best fit for $P_s(0) = 1$. The best fit for $P_f(0)$ was always independent of constraints and was >0.4. $P_f(0)$ was generally smaller for the two mutations.

RESULTS

Single Channel Recordings

Single channel recordings of the Cl^- channel ClC-0 from *Torpedo* are characterized by an apparent "double-pore" behavior in which relatively long closures separate bursts of activity during which the channel opens stochastically to two nonzero, equidistant conductance levels (Miller, 1982; Miller and Richard, 1990; Chen and Miller, 1996; Ludewig et al., 1997). Single-channel studies of ClC-1 (Steinmeyer et al., 1991b) are more difficult due to ClC-1's low conductance (Pusch et al., 1994; Wollnik et al., 1997) and fast gating (Pusch et al., 1994; Fahlke et al., 1996; Rychkov et al., 1996, 1998). Low intracellular pH (pH_i) leads to a slowing of gating kinetics and to an increase of the residual open probability at negative voltages (Rychkov et al., 1996). This effect of intracellular pH is illustrated in Fig. 1. We have exploited both effects to resolve single channel events of ClC-1 at low pH_i.

To this end, ClC-1 was expressed in *Xenopus* oocytes and we recorded currents from membrane micropatches using the inside-out configuration of the patch-

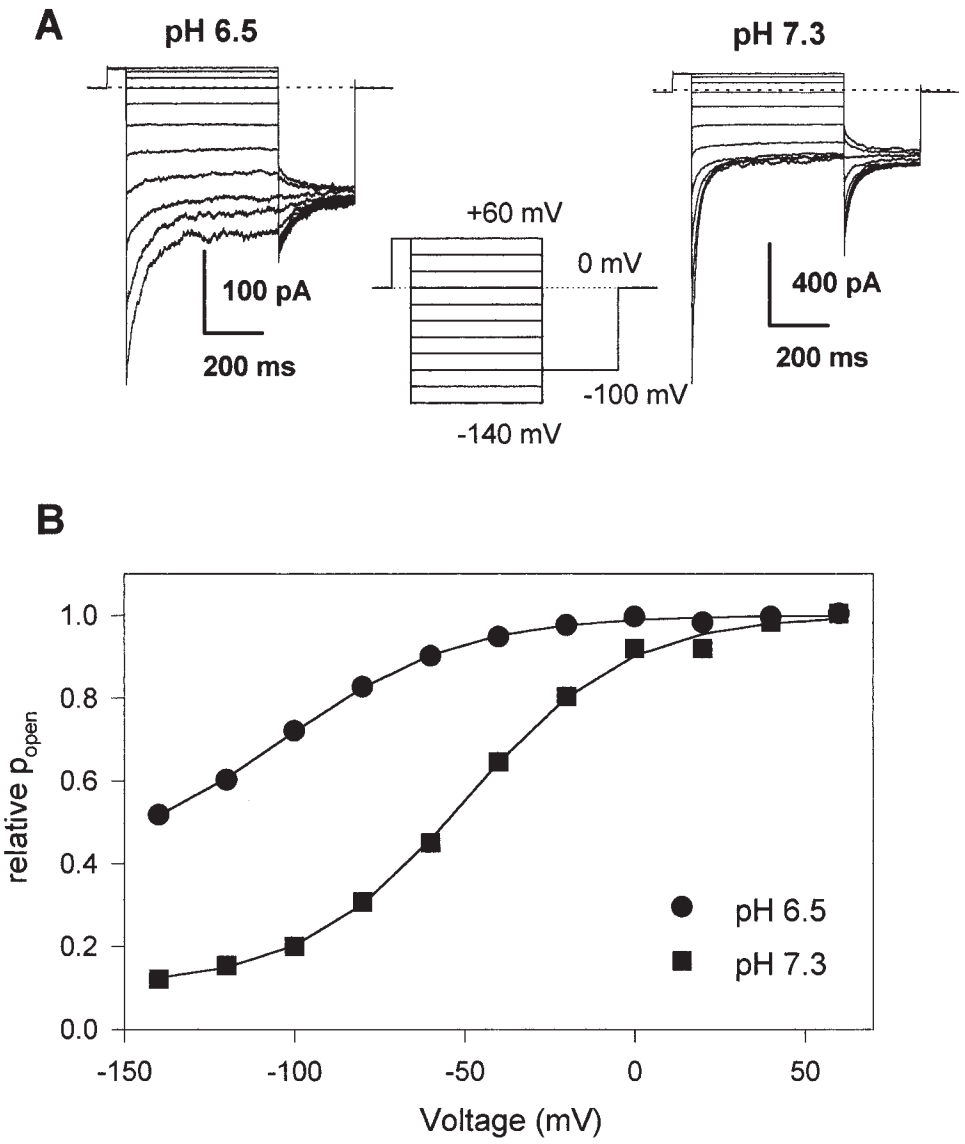

FIGURE 1. Effect of low intracellular pH on macroscopic gating of ClC-1. (A) Families of voltage-clamp traces measured from different inside-out patches in solutions with the indicated pH_i using the stimulation protocol shown in the inset. (B) Plot of the apparent steady state open probability at the end of the third segment of stimulation at different voltages measured as the initial tail current for the constant step to −100 mV normalized to the tail current after the prepulse to +60 mV.

clamp technique (Hamill et al., 1981) and pH 6.5 in the bath (internal) solution. To search for single-channel events, we first used relatively large-tipped patch-pipettes (resistance of 1–3 MΩ) to identify a region of the oocyte with significant but not too high expression. We then patched the same region of the oocyte membrane using pipettes with smaller tip openings (resistance of 4–8 MΩ). In a few patches ($n = 9$), we succeeded in obtaining recording conditions (high seal resistance, low background noise, and relatively long stability) allowing fairly clear resolution of single-channel events (Fig. 2 A). These records showed invariably two approximately equidistant open conductance levels easily distinguishable above the background noise at voltages between −100 and −140 mV. From Fig. 2 A, another important qualitative feature can be observed; i.e., fairly common closing periods separate bursts of openings that almost invariably contain both conductance levels. This behavior is similar to that of ClC-0 channels (Miller, 1982; Miller and Richard, 1990) and has been modeled as arising from the gating transitions of a double-pore channel with an independent parallel modulation by a common gate.

Amplitude histograms of long recordings confirm these qualitative observations. The histograms are very well fitted by the sum of three gaussian distributions with equidistant peaks ($i_0 \equiv 0$, i_1, $2i_1$) and additive variances (σ_0^2, $\sigma_0^2 + \sigma^2$, $\sigma_0^2 + 2\sigma^2$) as explained in METHODS (Fig. 2 B). Accordingly, the relative areas covered by the three gaussian components yield the probabilities P_0, P_1, and P_2 of the closed and of the two open levels, respectively (Fig. 2 C). A simple analysis shows that the values of the probabilities are grossly departing from the expectations from a simple binomial superposition

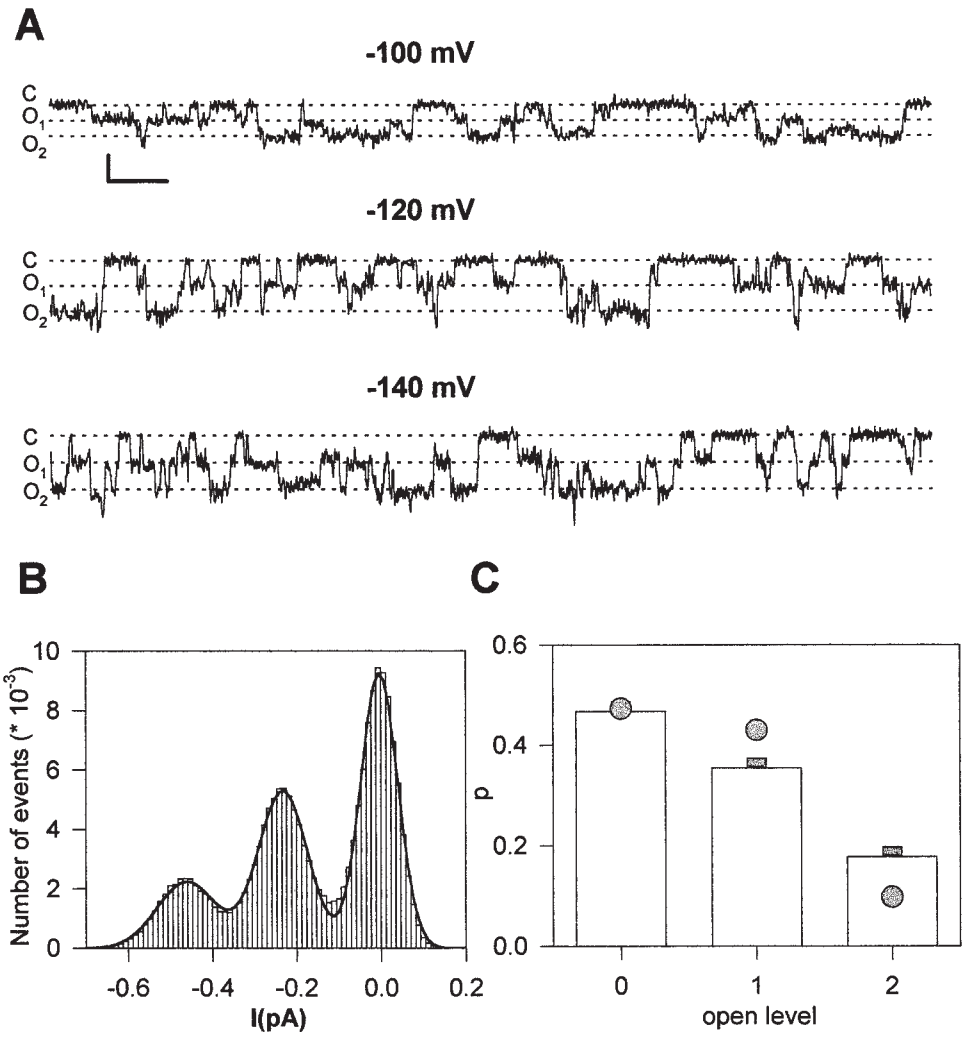

FIGURE 2. Single ClC-1 channels. (A) Single channel traces at different membrane potentials measured at pH_i 6.5. Only short segments of longer registrations are shown. Filtered at 100 Hz for display. For the analysis, data were filtered at 200 Hz (scale bars: 0.2 pA and 0.2 s). (B) Amplitude histogram of a registration at −140 mV and fit with the sum of three equidistant gaussian distributions. (C) Stationary probabilities for the three conductance levels obtained from the gaussian fit (boxes). Circles indicate the best fit assuming two independent channels each with open probability $P = 0.31$. The "raw" open probability, P_{raw}, obtained by integrating the baseline-subtracted raw current trace [$P_{raw} = <I>/(2i)$] was $P_{raw} = 0.36$ for the same data and yielded an even worse fit of the amplitude histogram (not shown). Squares represent the predictions assuming Fig. 3 B for a double-barreled channel with open probabilities $P_s = 0.71$ and $P_f = 0.50$, respectively, for the common gate and for the single protopore gate.

of two independently gating channels each with open probability P (Fig. 2 C, circles). Therefore, it can be excluded that the two open conductance levels are due to the presence of two identical and independent channels, and the invariable presence of both levels in all patches forces the conclusion that our recordings of the type shown in Fig. 2 A represent a single channel that has two open states, one with twice the conductance of the other. Based on the stationary probabilities obtained from the amplitude histograms, a model with two independently gated and equally sized conductances with possibly different open probabilities P_A and P_B, respectively (Fig. 3 A), can be excluded. Best fits of such a model to experimental amplitude histograms invariably yielded $P_A = P_B$, and thus the same bad prediction as the binomial superposition of two identical channels (Fig. 2 C, circles).

One long registration at −140 mV from a patch containing a single channel (Fig. 4 A) allowed us to perform a fair statistical analysis of dwell times (Fig. 4 B). This showed that histograms of single- and double-opening times were well fitted by single exponential distributions, whereas a single exponential was inadequate to fit the closed time histogram (Fig. 4 B, top, dashed line).

A model that can account for our observations must include a common gate that modulates the access to a conduction pathway that can have three different conductances (0, γ, 2γ). The simplest kinetic scheme (with the smallest number of parameters) is shown in Fig. 3 B. The three conductance levels of the "open" common gate are modeled by a binomial superposition of two equal and independent processes. The kinetic scheme can be mechanistically interpreted according to either one of the models shown in Fig. 3 (C or D). Fig. 3 C assumes the classical double-barreled structure where Cl^- has equal access to two parallel, equal and, independent two-state protopores (Miller, 1982). In Fig. 3 D, Cl^- is allowed by the common gate to enter a single permeation pathway that, however, can assume three different conformations. As discussed later, there are several arguments in favor of either interpretation, but it is important to stress that both lead to

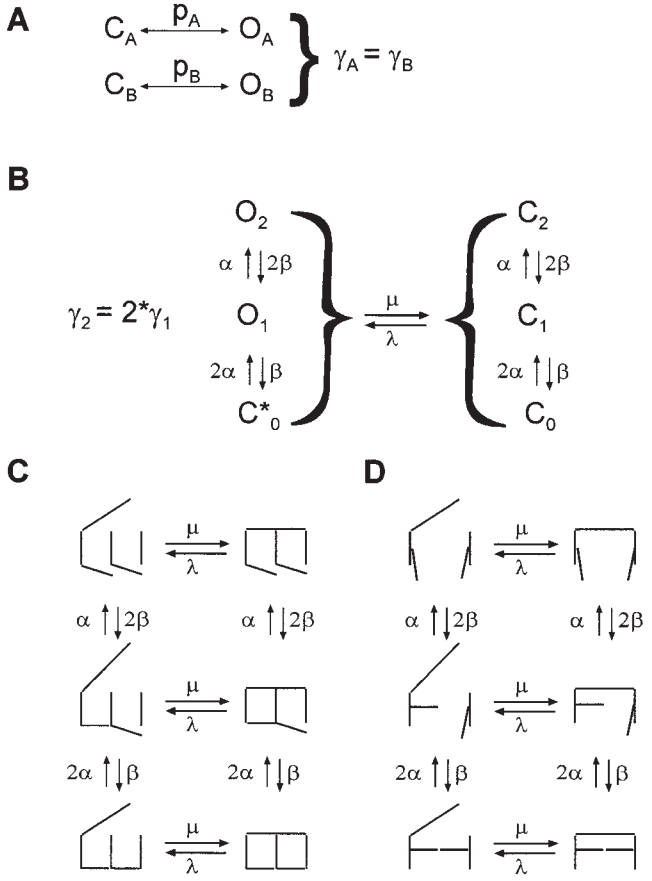

FIGURE 3. Possible kinetic schemes and models describing ClC-1 gating. A represents a double-barreled channel with two different fast gates but no common slow gate. B incorporates two independent types of "gates," a slow common gate and two independent fast gates. Two different interpretations of this kinetic scheme are shown in C and D. In the model originally proposed for ClC-0 (Miller, 1982; Miller and Richard, 1990), two equal, independent two-state protopores are modulated simultaneously by a common gate (C). In the model shown in D, a single permeation pathway has three equidistant subconductance states that are binominally distributed.

the very same kinetic scheme. For analogy with ClC-0, we adopt in the following the interpretation and terminology of the double-pore model (Fig. 3 C) for describing the data in terms of the kinetic scheme of Fig. 3 B.

The simple double-barreled model is characterized by the single-protopore open probability P_f, a probability P_s for the opening of the common slow gate, and the independence of the two gating processes. It can reproduce exactly the stationary probabilities of the three conductance levels obtained from the amplitude histograms using the relationships:

$$P_0 = 1 - P_s + P_s*(1 - P_f)^2;\ P_1 = 2*P_s*P_f*(1 - P_f);\ P_2 = P_s*P_f^2;\ P_0 + P_1 + P_2 = 1$$

(Fig. 2 C, squares). The exact fit of the data does not demonstrate the model because we have two parameters and two independent data points. However, the consistency of the values of P_f, P_s, and γ with other measurements can be used as a more stringent test of its validity. Firstly, the single channel currents give a conductance γ of 1.2–1.3 pS for each protopore (Fig. 5 C, left, ●), which is in good agreement with previous (Pusch et al., 1994; Wollnik et al., 1997; Rychkov et al., 1998) and present noise analysis (see below) of macroscopic currents clearly attributable to ClC-1 channels. This also supports the assumption that the events indeed represent openings of ClC-1 and not endogenous channels. Furthermore, both P_s and P_f (Fig. 5 C, ●) are only a little voltage dependent in the small voltage range investigated and have values well above 0.5, that are consistent with the macroscopic activation curve of ClC-1 at pH_i 6.5 (Rychkov et al., 1996; Fig. 1).

The double-barreled model (Fig. 3) is also consistent with our measurements of dwell-time distributions, since it predicts in particular single exponential dwell-time distributions for both open levels and a multiexponential distribution for the closed times (the theory predicts four exponentials, but major contributions are only from two components). To obtain best estimates for the four rate constants in Fig. 3 B, the dwell-time histograms were fitted simultaneously according to the double-barreled model using maximum likelihood techniques (see METHODS). The histograms are well fitted (Fig. 4 B, solid lines) with the rate constants given in the legend to Fig. 4. From the rate constants, the stationary probabilities can be calculated as $P_f = \alpha/(\alpha + \beta) = 0.59$ and $P_s = \lambda/(\lambda + \mu) = 0.68$. These values are close to those obtained independently from the amplitude histogram of the same patch ($P_f = 0.48$, $P_s = 0.74$), supporting further the validity of the double-barreled model. We notice that, while the relaxation time constant of the fast gate, τ_f [defined as $1/(\alpha + \beta)$], is similar to that of ClC-0 at −100 mV, that of the slow gate, τ_s [defined as $1/(\lambda + \mu)$], is less than three times larger and more than two orders of magnitude smaller than for ClC-0 (Pusch et al., 1997; our unpublished results) making the dissection of the two gating processes much more difficult. These two time constants of gating probably correspond to the two macroscopic time constants of current deactivation described by Fahlke et al. (1995, 1996) and Rychkov et al. (1996) that also differ by a factor of 3–5.

In contrast to their qualitative similarities in showing two equally spaced conductance levels, a major difference in the gating properties of ClC-1 and ClC-0 is the different voltage dependence of the slow gating mechanism. In ClC-0, the slow gate closes at positive voltages leading to a small steady state macroscopic conductance in the positive voltage range. In contrast, in ClC-1,

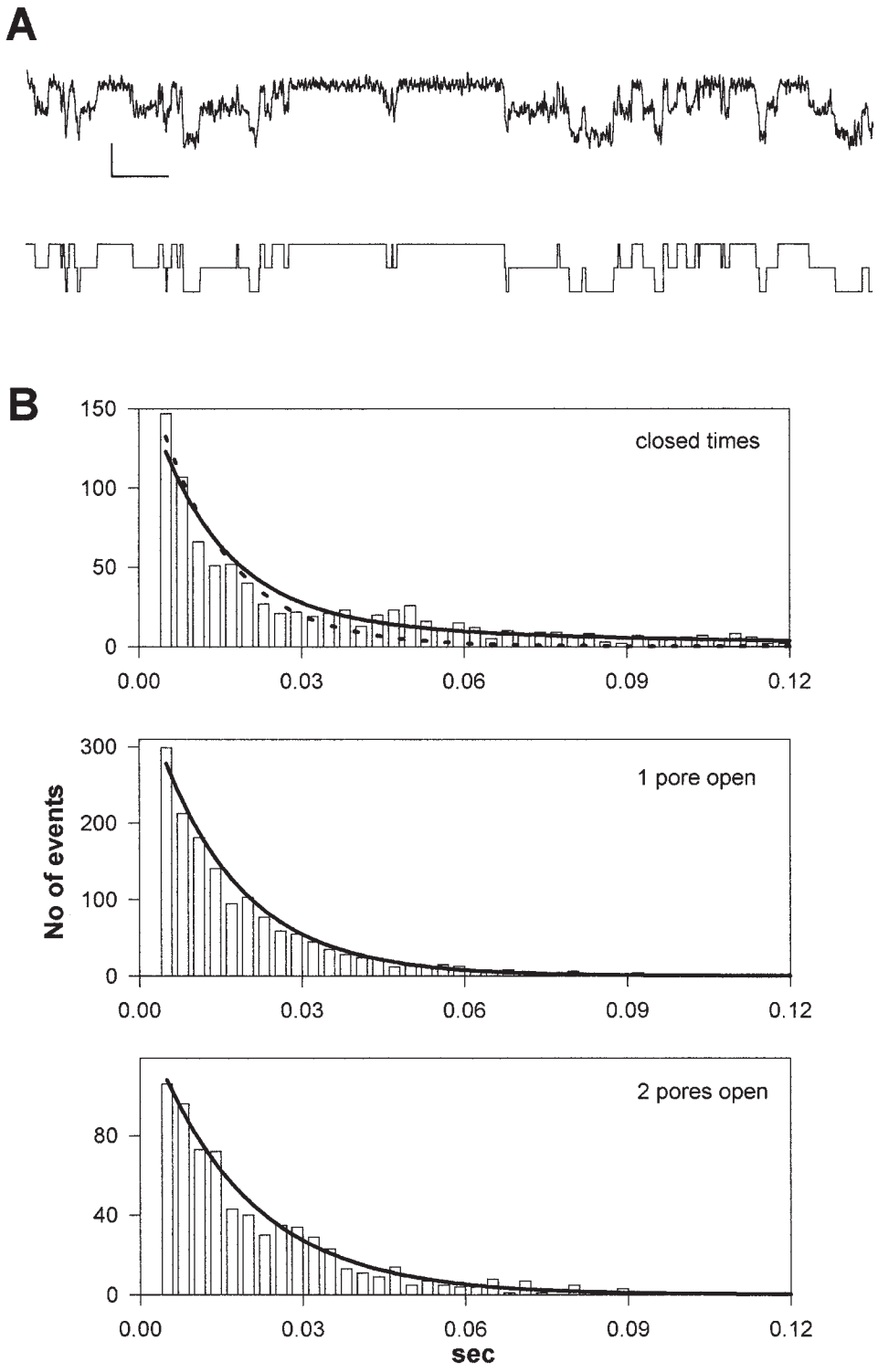

FIGURE 4. Kinetic analysis of a particularly clean recording. (A) Short segment of the original registration filtered at 200 Hz (top) and the corresponding idealized trace (bottom; scale bars: 0.3 pA and 0.1 s). (B) Dwell time histograms for the three conductance levels (boxes). The dashed line in the top panel is a single exponential fit to the closed-time histogram. Solid lines represent a combined fit of the model shown in Fig. 3 B to the histograms using the maximum-likelihood criterion. Values for the rate constants obtained from the fit are (s^{-1}): α, 34; β, 22; λ, 13; μ, 6. From these, the stationary probabilities $P_f = \alpha/(\alpha + \beta) = 0.59$ and $P_s = \lambda/(\lambda + \mu) = 0.68$, and the relaxation times $\tau_f = 1/(\alpha + \beta) = 17$ ms and $\tau_s = 1/(\lambda + \mu) = 51$ ms can be calculated with a ratio $\tau_s/\tau_f < 3$. The stationary probabilities obtained from the amplitude histogram of the same patch are $P_f = 0.48$, $P_s = 0.74$.

the overall steady state conductance increases monotonically with increasing voltage (Pusch et al., 1994; Rychkov et al., 1996; Fig. 1), implying that the slow gate remains open at positive voltages. From the noise analysis described below, it appears that the open probability of the slow gate approaches a value of 1 at positive voltages, indicating that the slow gate has a reversed voltage dependence in ClC-1 compared with ClC-0. However, several point mutations of ClC-0 also lead to a loss of voltage sensitivity (Ludewig et al., 1996) or even a reversed voltage dependence of the slow gate (our unpublished results).

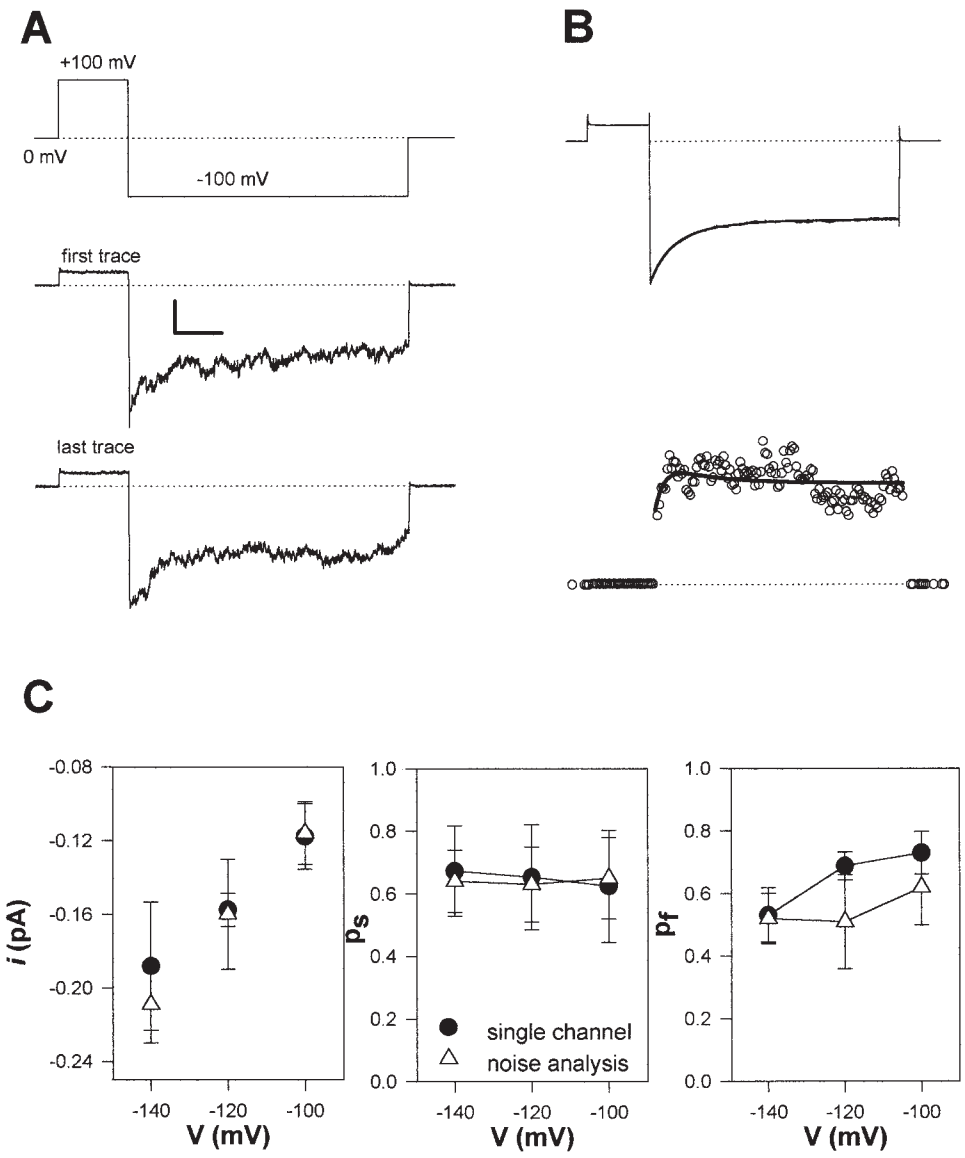

FIGURE 5. Determination of single channel parameters using macroscopic fluctuation analysis. (A) The voltage protocol (top) was applied repeatedly (at least 100 times). Representative individual registrations are shown below (pH_i 6.5; scale bars: 0.1 s and 4 pA). (B) Mean current response for the step to −100 mV (top) and corresponding variance (see METHODS; scale bar: 0.3 pA^2). Thick solid lines represent kinetic fits assuming independent single-exponential gating relaxations for the two gates as described in METHODS. For clarity, averages of 10 data points are shown as circles for the experimental variance. For the fit, no averaging was performed. (C) Comparison of mean values for the single channel current, i, and the stationary open probabilities, P_s and P_f, obtained by the fluctuation analysis (△: −140 mV, n = 8; −120 mV, n = 11; −100 mV, n = 9) with the values obtained from the amplitude histograms of single-channel recordings (●: −140 mV, n = 4; −120 mV, n = 7; −100 mV, n = 4).

Macroscopic Current Fluctuations

To extend our studies to physiological pH conditions in which the faster kinetics prevent the recordings of single channel events, we developed a method to estimate P_f and P_s from macroscopic current fluctuations. The method is illustrated in Fig. 5 for measurements at pH_i 6.5, and the analysis procedure is described in detail in the METHODS. From repeated stimulations (Fig. 5 A), the time course of the mean current and of its variance were calculated (Pusch et al., 1994) (Fig. 5 B) and fitted with Eqs. 2 and 3. The best fitting values of P_f, P_s, and i thus obtained were consistent with those measured from the single-channel amplitude histograms (Fig. 5 C; compare ● and △). As already mentioned, this good accordance of the single channel analysis and the fluctuation analysis supports the assumption that the single-channel events described above are indeed due to ClC-1 channels and not to endogenous oocyte channels. Vice versa, it justifies the use of macroscopic fluctuation analysis for estimating the single channel parameters of our model.

Myotonic Mutations

Mutations of ClC-1 can cause either dominant or recessive myotonia (Steinmeyer et al., 1991a, 1994; Koch et al., 1992; George et al., 1993; Pusch et al., 1995b). Recessive myotonia is frequently associated with mutations leading to a partial or total loss of function (see Jentsch and Günther, 1997). This is consistent with the in vitro result that a reduction of the macroscopic muscle Cl^- conductance by 50% is not sufficient to cause myotonia (Kwiecinski et al., 1988). Several dominant mutations

(as for example mutation I290M) lead to a large shift of the conductance–voltage curve to positive voltages of homomeric channels that is only partially reduced in wild-type (WT)/mutant heteromers, leaving a strong reduction of the chloride conductance at the relevant physiological voltages (Pusch et al., 1995b).

Recently, mutations that cause either recessive myotonia or a benign form of dominant myotonia with incomplete penetrance have been identified (Plassart-Schiess et al., 1998) that show a positive shift of the macroscopic conductance–voltage relationship in homodimeric mutant channels, but form mutant/WT heterodimers that behave almost like homomeric WT channels (Kubisch et al., 1998). An example of these mutations that do not impose the shift on WT/mutant heteromers is the mutation I556N (Kubisch et al., 1998). The different behavior of mutant/WT heteromeric channels indicates that the mechanism underlying the shift of the conductance–voltage curve of mutants I290M and I556N is different.

To investigate whether these two mutations produce different effects on the two gates postulated by Fig. 3 B, we used macroscopic fluctuation analysis at the physiological pH_i 7.3 to estimate and compare the values of γ and of the stationary probabilities for WT and mutants I290M and I556N (Fig. 6). The WT value of γ at pH_i 7.3 was not significantly different from that at pH_i 6.5, and γ was also not significantly affected by the mutations. The WT estimates of P_f and P_s at −100 mV were smaller at pH_i 7.3 than at pH_i 6.5, consistent with the effect of pH_i on the macroscopic conductance (Rychkov et al., 1996; Fig. 1). The relative macroscopic open probability (Fig. 1) compares well with the calculated product $P_f{*}P_s$ from the noise analysis at both pH_i values (not shown), indicating that P_f as well as P_s approach 1 at large positive voltages. Also, the initial values [$P_f(0)$, $P_s(0)$] obtained from the noise analysis were close to 1 in most cases (see METHODS). For the same pH_i 7.3 conditions, the estimated stationary open probabilities were both significantly reduced by the mutations (Fig. 6 B). In particular, mutant I290M shows a significantly larger reduction of P_s than mutant I556N, whereas both mutations cause a similar reduction of P_f.

DISCUSSION

We presented in this work some new information that is relevant for the modeling of the gating mechanism

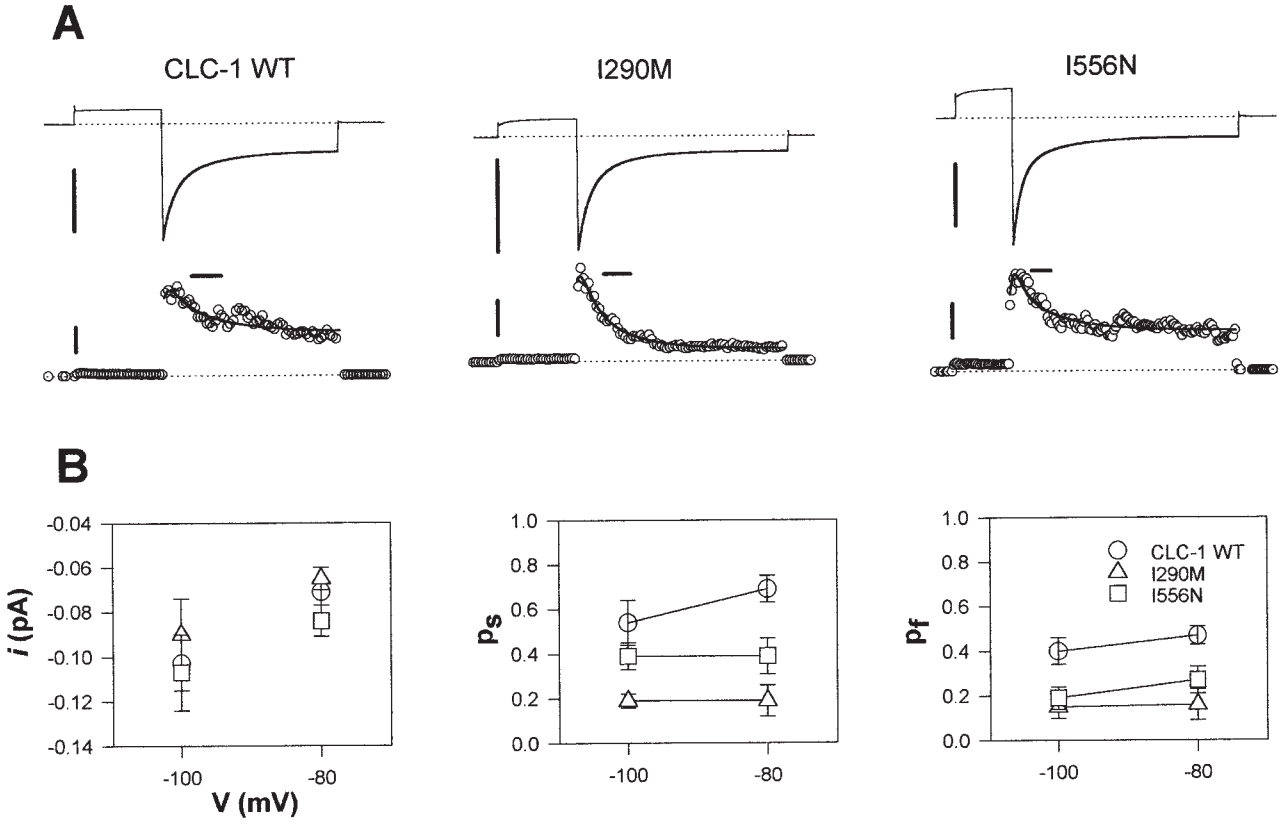

FIGURE 6. Fluctuation analysis for WT ClC-1 and the myotonic mutations I290M and I556N. (A) Representative fluctuation analysis for the three channel types. Mean current (top) and variance (bottom) are shown together with the kinetic fits (thick lines; see Fig. 5). (Registrations are at −100 mV, pH_i 7.3; horizontal scale bars, 50 ms; vertical scale bars, 200 pA [top] and 5 pA^2 [bottom].) (B) Comparison of single channel parameters obtained for WT ClC-1 and mutants I290M and I556N at pH_i 7.3.

of the muscle Cl^- channel ClC-1. Our single-channel recordings show that the gating of this channel has strong similarities with that of the "classical" ClC prototype ClC-0, although the slow common gate of ClC-1 has faster kinetics and a different voltage dependence. Therefore, we have assumed that many of the arguments suggesting that ClC-0 channels have a double-barreled structure apply also to ClC-1, and we have used a simple kinetic scheme involving a common gate on top of two parallel and independently gated pores to fit our single-channel data. We have also shown that the analysis of macroscopic current fluctuations on the basis of that scheme gives consistent estimates of the single-channel parameters. Macroscopic fluctuation measurements were then used to characterize two ClC-1 mutants linked to hereditary myotonias. Such analysis supports the simple mechanistic hypothesis of Kubisch et al. (1998) for the different inheritance pattern of the two mutations in terms of the two-gate double-barreled model: monomers of the recessive mutant I556N may associate with WT subunits to form fairly functional dimers because only the protopore provided by the mutant subunit has strongly modified properties, whereas monomers of the dominant mutant I290M modify both homodimers and mutant/WT heterodimers because they affect the common gate.

To what extent do our results support the hypothesis of a double-barreled structure of ClC-1? The fact that our single-channel recordings are consistent with the simple kinetic scheme of Fig. 3 B does not exclude the possibility that more complicated gating schemes are needed for a quantitative description of ClC-1 gating in a wider range of voltage, in different ionic conditions, and at a higher time resolution. Due to their small conductance and relatively fast kinetics, single ClC-1 channels can be observed with much less resolution than ClC-0 (Ludewig et al., 1996, 1997; Chen and Miller, 1996; Middleton et al., 1996), and the argument in favor of an apparent double-barreled structure is correspondingly weaker. In particular, the relative kinetic overlap of the fast and slow gates makes their distinction more difficult. Since ClC-0 and ClC-1 are structurally very similar (Jentsch et al., 1990; Steinmeyer et al., 1991b) and have several common permeation and gating properties (e.g., Miller and Richard, 1990; Pusch et al., 1995a; Rychkov et al., 1996, 1998; Ludewig et al., 1997; for review see Pusch and Jentsch, 1994; Foskett, 1998) our finding that they also show the same basic subconductance behavior further supports the idea that these two channels share similar structure–function relationships.

Recently, Fahlke et al. (1998) suggested that ClC-1 has only one pore and supported this hypothesis with measurements of the effect on macroscopic currents of various channel-modifying reagents in homo- and heteromeric ClC-1 mutant constructs. With the assumption that the reagents act by a pore-blocking mechanism, they interpret their results as incompatible with a channel structure with two physically distinct conduction pathways. This conclusion would be hard to extend to ClC-0 channels, for which the evidence for the presence of two physically distinct conduction pathways, based on mutagenesis and single-channel recordings, is very strong (Middleton et al., 1996; Ludewig et al., 1996).

Almost symmetric subconductance states have also been observed in other channel types that are definitively single-barreled channels (e.g., Root and MacKinnon, 1994). Root and MacKinnon (1994) observed independent protonation of two identical sites that led to the appearance of binomially distributed subconductance states in a cyclic nucleotide–gated cation (CNG) channel. Such a mechanism is similar to the interpretation of ClC-1 gating as shown in Fig. 3 D, even though the gating of the CNG channel is different from ClC-0/ClC-1 gating in at least two aspects: (a) the subconductance states in the CNG channel are not equidistant and (b) the lowest conductance state with an open "common" gate is not zero in the CNG channel. Most importantly, however, the results of Middleton et al. (1996) and Ludewig et al. (1996) for ClC-0 are extremely difficult to explain on the basis of a channel with a single pore: in these studies, the conductance, ion selectivity, and gating properties of single protopores could be altered independently from the other protopore, resulting in heteromeric asymmetric double-barreled channels in which the properties of the two protopores were identical to those of the respective homomeric parent channels.

On the other hand, we argue that the results of Fahlke et al. (1998) for ClC-1 can also be easily interpreted in the framework of a double-barreled channel. First, it has not been ruled out by Fahlke et al. (1998) that the reagents used in their study decrease the macroscopic current amplitude not by a pore-blocking mechanism, but by acting on the gating of the channel. In the voltage-dependent sodium channel, for example, amino acids of the "S4 segment" that probably do not contribute to the pore are accessible to cysteine-modifying reagents, and their modification leads to persistent changes in gating properties (e.g., Yang et al., 1997). The fact that some of the cysteine substitutions, used by Fahlke et al. (1998) to make the channels sensitive to the modifying reagents, do per se modify drastically the macroscopic currents mediated by ClC-1, suggests that this could indeed be the case. If, for example, the effect of the cysteine substitution is on the common gate, it is plausible that the ulterior modification produced by the binding of MTSES [sodium (2-sulfonatoethyl)methanethiosulfonate] (or other reagents)

forces this gate into a closed conformation. This would explain the results of Fahlke et al. (1998), which would then be fully compatible with a double-barreled model. In addition, even accepting the pore-blockage assumption, it could be that the two pores of the channel have common intracellular and/or extracellular vestibules and that the modifying reagents act by blocking in these regions the entrance to both pores simultaneously.

In conclusion, our present data demonstrate that single ClC-1 channels behave like ClC-0 channels. Therefore, considering that the basic molecular structure of both channels is similar and, in the absence of more compelling evidence to the contrary, we maintain our preference for the idea that both channels are characterized by a double-barreled structure with two identical and physically distinct conduction pathways. In fact, we think that future observations will likely establish the notion of the double barrel as a distinctive common motif of the structure of all ClC channels, some of which have functional properties that are very poorly understood except for their involvement in hereditary diseases like kidney stone diseases (Lloyd et al., 1996) and Bartter's syndrome (Simon et al., 1997).

We thank T.J. Jentsch for kindly providing the cDNAs and for sharing unpublished material.
This study was partially supported by Telethon, Italy (grants 926 and 1079).

Original version received 25 November 1998 and accepted version received 22 January 1999.

REFERENCES

Colquhoun, D., and A.G. Hawkes. 1995. A Q-matrix cookbook. *In* Single-Channel Recording. 2nd ed. B. Sakmann and E. Neher, editors. Plenum Publishing Corp., New York. 589–633.

Chen, T.Y., and C. Miller. 1996. Nonequilibrium gating and voltage dependence of the ClC-0 Cl^- channel. *J. Gen. Physiol.* 108:237–250.

Conti, F. 1984. Noise analysis and single-channel recordings. *Curr. Top. Membr. Transp.* 22:371–405.

Fahlke, C., T.H. Rhodes, R.R. Desai, and A.L. George, Jr. 1998. Pore stoichiometry of a voltage-gated chloride channel. *Nature.* 394:687–690.

Fahlke, C., R. Rüdel, N. Mitrovic, M. Zhou, and A.L. George, Jr. 1995. An aspartic residue important for voltage-dependent gating of human muscle chloride channels. *Neuron.* 15:463–472.

Fahlke, C., A. Rosenbohm, N. Mitrovic, A.L. George, and R. Rüdel. 1996. Mechanism of voltage-dependent gating in skeletal muscle chloride channels. *Biophys. J.* 71:695–706.

Foskett, J.K. 1998. ClC and CFTR chloride channel gating. *Annu. Rev. Physiol.* 60:689–717.

George, A.L., Jr., M.A. Crackower, J.A. Abdalla, A.J. Hudson, and G.C. Ebers. 1993. Molecular basis of Thomsen's disease (autosomal dominant *myotonia congenita*). *Nat. Genet.* 3:305–310.

Hamill, O.P., A. Marty, E. Neher, B. Sakmann, and F.J. Sigworth. 1981. Improved patch clamp techniques for high-resolution current recording from cells and cell-free membrane patches. *Pflügers Arch.* 391:85–100.

Jentsch, T.J., and W. Günther. 1997. Chloride channels: an emerging molecular picture. *Bioessays.* 19:117–126.

Jentsch, T.J., K. Steinmeyer, and G. Schwarz. 1990. Primary structure of *Torpedo marmorata* chloride channel isolated by expression cloning in *Xenopus* oocytes. *Nature.* 348:510–514.

Kubisch, C., T. Schmidt-Rose, B. Fontaine, A.H. Bretag, and T.J. Jentsch. 1998. ClC-1 chloride channel mutations in myotonia congenita: variable penetrance of mutations shifting the voltage-dependence. *Hum. Mol. Genet.* 7:1753–1760.

Kwiecinski, H., F. Lehmann-Horn, and R. Rüdel. 1988. Drug-induced myotonia in human intercostal muscle. *Muscle Nerve.* 11: 576–581.

Koch, M.C., K. Steinmeyer, C. Lorenz, K. Ricker, F. Wolf, M. Otto, B. Zoll, F. Lehmann-Horn, K.H. Grzeschik, and T.J. Jentsch. 1992. The skeletal muscle chloride channel in dominant and recessive human myotonia. *Science.* 257:797–800.

Lloyd, S.E., S.H. Pearce, S.E. Fisher, K. Steinmeyer, B. Schwappach, S.J. Scheinman, B. Harding, A. Bolino, M. Devoto, P. Goodyer, et al. 1996. Mutations in the chloride channel ClC-5 are associated with X-linked hypercalciluric nephrolithiasis. *Nature.* 379:445–449.

Ludewig, U., M. Pusch, and T.J. Jentsch. 1996. Two physically distinct pores in the dimeric ClC-0 channel. *Nature.* 383:340–343.

Ludewig, U., M. Pusch, and T.J. Jentsch. 1997. Independent gating of single pores in ClC-0 chloride channels. *Biophys. J.* 73:789–797.

Middleton, R.E., D.J. Pheasant, and C. Miller. 1996. Homodimeric structure of a ClC-type channel. *Nature.* 383:337–340.

Miller, C. 1982. Open-state substructure of single chloride channels from *Torpedo* electroplax. *Phil. Trans. R. Soc. Lond. B Biol. Sci.* 299:401–411.

Miller, C., and E.A. Richard. 1990. The voltage-dependent chloride channel of *Torpedo electroplax*. Intimations of molecular structure from quirks of single-channel function. *In* Chloride Channels and Carriers in Nerve, Muscle, and Glial Cells. F.J. Alvarez-Leefmans and J.M. Russell, editors. Plenum Publishing Corp., New York. 383–405.

Plassart-Schiess, E., A. Gervais, B. Eymard, A. Lagueny, J. Pouget, J.M. Warter, M. Fardeau, T.J. Jentsch, and B. Fontaine. 1998. Novel muscle chloride channel (ClCN1) mutations in myotonia congenita with various modes of inheritance including incomplete dominance and penetrance. *Neurology.* 50:1176–1179.

Pusch, M., and T.J. Jentsch. 1994. Molecular physiology of voltage-gated chloride channels. *Physiol. Rev.* 74:813–827.

Pusch, M., U. Ludewig, and T.J. Jentsch. 1997. Temperature dependence of fast and slow gating relaxations of ClC-0 chloride channels. *J. Gen. Physiol.* 109:105–116.

Pusch, M., U. Ludewig, A. Rehfeldt, and T.J. Jentsch. 1995a. Gating of the voltage-dependent chloride channel ClC-0 by the permeant anion. *Nature.* 373:527–531.

Pusch, M., K. Steinmeyer, and T.J. Jentsch. 1994. Low single channel conductance of the major skeletal muscle chloride channel, ClC-1. *Biophys. J.* 66:149–152.

Pusch, M., K. Steinmeyer, M.C. Koch, and T.J. Jentsch. 1995b. Mutations in dominant human myotonia congenita drastically alter the voltage-dependence of the ClC-1 chloride channel. *Neuron.* 15:1455–1463.

Root, M.J., and R. MacKinnon. 1994. Two identical noninteracting sites in an ion channel revealed by proton transfer. *Science.* 265: 1852–1856.

Rychkov, G.Y., M. Pusch, D.St.J. Astill, M.L. Roberts, T.J. Jentsch, and A.H. Bretag. 1996. Concentration and pH dependence of skeletal muscle chloride channel ClC-1. *J. Physiol. (Camb.).* 497: 423–435.

Rychkov, G.Y., M. Pusch, M.L. Roberts, T.J. Jentsch, and A.H. Bretag. 1998. Permeation and block of the skeletal muscle chloride channel, ClC-1, by foreign anions. *J. Gen. Physiol.* 111:653–665.

Simon, D.B., R.S. Bindra, T.A. Mansfield, C. Nelson-Williams, E. Mendonca, R. Stone, S. Schurman, A. Nayir, H. Alpay, A. Bakkaloglu, et al. 1997. Mutations in the chloride channel gene, ClCNKB, cause Bartter's syndrome type III. *Nat. Genet.* 17:171–178.

Steinmeyer, K., R. Klocke, C. Ortland, M. Gronemeier, H. Jockusch, S. Gründer, and T.J. Jentsch. 1991a. Inactivation of muscle chloride channel by transposon insertion in myotonic mice. *Nature.* 354:304–308.

Steinmeyer, K., C. Ortland, and T.J. Jentsch. 1991b. Primary structure and functional expression of a developmentally regulated skeletal muscle chloride channel. *Nature.* 354:301–304.

Steinmeyer, K., M. Pusch, M.C. Koch, and T.J. Jentsch. 1994. Multimeric structure of ClC-1 chloride channel revealed by mutations in dominant myotonia congenita (Thomsen). *EMBO (Eur. Mol. Biol. Organ.) J.* 13:737–743.

Wollnik, B., C. Kubisch, K. Steinmeyer, and M. Pusch. 1997. Identification of functionally important regions of the muscular chloride channel ClC-1 by analysis of recessive and dominant myotonic mutations. *Hum. Mol. Genet.* 6:805–811.

Yang, N., A.L. George, and R. Horn. 1997. Probing the outer vestibule of a sodium channel voltage sensor. *Biophys. J.* 73:2260–2268.